Fruit Research

ARTICLE

Open Access

https://doi.org/10.48130/frures-0025-0010

Fruit Research **2025**, 5: e021

Characterisation of early fruit development-specific miRNAs and their targets in peach using small RNA and degradome sequencing

Yanping Zhang[1*], Xudong Zhu[2], Chen Wang[3] and Mengqing Ge[1]

[1] *Suzhou Polytechnic Institute of Agriculture, Suzhou 215008, Jiangsu, China*
[2] *Subtropical Agriculture Research Institute, Fujian Academy of Agricultural Sciences, Zhangzhou 363005, Fujian, China*
[3] *College of Horticulture, Nanjing Agricultural University, Nanjing 210095, Jiangsu, China*
* Corresponding author, E-mail: ypzhang@szai.edu.cn

Abstract

Peach (*Prunus persica* L.) is a key drupe fruit crop characterized by a double-sigmoid growth pattern during fruit development. MicroRNAs (miRNAs) play pivotal regulatory roles in this process; however, their functions in early peach fruit development remain poorly understood. To address this, we conducted high-throughput small RNA (sRNA) sequencing at three critical developmental stages: 20, 50, and 75 d post-anthesis (DPA20, DPA50, DPA75), representing exponential growth, lag phase, and rapid regrowth, respectively. We identified 124 known miRNAs from 70 families and 86 novel miRNAs, with 97 and 79 miRNAs differentially expressed between DPA50 vs DPA20 and DPA75 vs DPA50, respectively. Degradome sequencing revealed 216 target genes for 74 known and eight novel miRNAs, with targets of ppe-miR160a and ppe-miR393b validated using RNA ligase-mediated rapid amplification of 5' cDNA ends (RLM-5'RACE). Quantitative reverse transcriptase polymerase chain reaction (qRT-PCR) confirmed the expression patterns of five miRNAs and their target genes, consistent with sequencing data. Network analysis revealed the involvement of the auxin signaling pathway and a complex miRNA regulatory network in fruit enlargement. Key miRNA-target interactions, such as ppe-miR160a-*ARF*s, ppe-miR172a/c/d-*AP2*s, ppe-miR166a -*ATHB*s, and ppe-miR319c/e-*TCP*s were implicated in cell proliferation and differentiation, with novel findings including ppe-miR171b/f/h-*SCL6*s in cell division. In summary, peach miRNAs primarily regulate early fruit growth and development by modulating auxin signaling and mediating cell division and differentiation. These findings provide critical insights into miRNA-mediated mechanisms underlying peach fruit development and establish a foundation for future research on drupe fruit crops.

Citation: Zhang Y, Zhu X, Wang C, Ge M. 2025. Characterisation of early fruit development-specific miRNAs and their targets in peach using small RNA and degradome sequencing. *Fruit Research* 5: e021 https://doi.org/10.48130/frures-0025-0010

Introduction

MicroRNAs (miRNAs) are small, endogenous, non-coding RNA molecules, typically 20–22 nucleotides (nt) in length, that play critical regulatory roles in various biological processes, including development, abiotic stress responses, signal transduction, and pathogen resistance[1–5]. Extensive studies have demonstrated that miRNAs are ubiquitous in plants and exhibit high conservation across species. To date, a large number of miRNAs have been identified and cataloged in miRBase (version 22.0), highlighting their essential functions in numerous metabolic processes, particularly fruit development[6–9]. For instance, overexpression of miR156b has been linked to abnormal fruit morphology in tomato plants[10]. Additionally, miR156/157 and miR172 have been shown to regulate tomato ripening by targeting key regulators such as *CNR* and *AP2*a. In strawberries, miR159a targets *FaGAMYB*, which is involved in the transition from receptacle development to ripening[11]. Similarly, miR73 modulates ABI5, a regulator of strawberry ripening through the ABA signaling pathway[12].

MiRNAs have been identified by predictive bioinformatics analyses and Sanger sequencing[13,14]. Recently, rapid developments in high-throughput sequencing have facilitated the application of transcriptome profiling in identifications in various fruit-producing species such as apple[15], grape[16,17], peach[18,19], pomegranate[20], date palm[21], sweet orange[22], and blue berry[23]. Similarly, degradome sequencing has revealed miRNA-mRNA target pairs which are prevalent during fruit development[15,22]. Moreover, the combination analyses of miRNAome and degradome have verified various roles of miRNAs during fruit development.

Peach (*Prunus persica* L.) is a highly valued deciduous fruit crop, prized for its delicious and nutritious fruit, and is widely cultivated in temperate regions worldwide. As a member of the Rosaceae family, which comprises over 3,000 species across approximately 110 genera[24]. Given their small genome size of approximately 300 Mb and relatively short reproductive time, peaches have been considered a plant genome model for Rosaceae[25,26]. The draft genome of peach (peach v2.0, derived from the 'Lovell' haploid) was sequenced by the International Peach Genome Initiative and is publicly accessible in the Genome Database for Rosaceae (www.rosaceae.org/peach/genome). Peach fruit development follows a typical double-sigmoid growth pattern[27], characterized by three distinct stages: an initial phase of exponential fruit size increase (FWI), a central lag phase with reduced growth rates (FWII), and a final phase of rapid regrowth (FWIII). Throughout these stages, the external appearance and internal physiological processes of the fruit undergo significant changes, with variations in fruit size, color, sugar content, organic acid levels, and hormone dynamics reflecting the expression profiles of specific genes and their regulators. Although miRNAs have been identified in various peach organs, including leaves, winter buds, roots, stems, flowers, and fruits[18,28–30], comprehensive analyses of miRNAs and their target genes across the three key stages of peach fruit development remain limited. Previous studies relied on a single mixed library to identify peach fruit miRNAs and their targets[18], underscoring the need for more detailed investigations[18].

In contrast to previous approaches, we utilized three sRNA libraries and their corresponding degradome libraries, each repre-

© The Author(s)

senting a distinct developmental stage, to identify and characterize miRNAs and their targets at each phase of peach fruit development. Furthermore, we conducted a comprehensive analysis of differentially expressed miRNAs and their targets across these stages. Our findings provide valuable insights into the regulatory roles of miRNAs in controlling peach fruit development, shedding light on the molecular mechanisms underlying this process.

Materials and methods

Plant materials and measurements of fruit parameters

After flowering, fruit samples were collected from 10-year-old 'Baifeng' peach trees cultivated under standard field conditions in Suzhou, China. Sampling was performed at 10, 20, 30, 40, 50, 63, 75, 87, and 95 days post-anthesis (DPA). Nine 'Baifeng' trees were evenly divided into three groups, with each group serving as a technical replicate containing three biological replicates. On each sampling date, single-bearing shoots were selected from each tree. The longitudinal and transverse diameters of the fruits were measured using vernier calipers, after which the pulp was separated, immediately snap-frozen in liquid nitrogen, and stored at −80 °C until further use.

Construction and sequencing of sRNA and degradome libraries

After identifying three key sampling points on the double-sigmoid growth curve of 'Baifeng' peaches, we selected DPA20, DPA50, and DPA75 as representative stages of FWI, FWII, and FWIII, respectively, for sRNA and degradome sequencing. Total RNA was extracted from fruit pulp samples at DPA20, DPA50, and DPA75 using TRIzol reagent (Invitrogen, CA, USA). RNA quality was assessed using an Agilent Bioanalyzer, and sample concentrations were determined with a Nanodrop Spectrophotometer. Subsequently, three sRNA and degradome libraries were constructed and subjected to single-end sequencing (50 bp) on an Illumina HiSeq 2500 platform (Illumina Inc., San Diego, CA, USA) at LC-BIO (Hangzhou, China). The raw sequencing data for small RNA and degradome libraries have been deposited in the NCBI Short Read Archive under the following accession numbers: DPA20-miRNAs (SRX4011348), DPA50-miRNAs (SRX4011349), DPA75-miRNAs (SRX4011350), DPA20-degradome (SRX4011351), DPA50-degradome (SRX4011352), and DPA75-degradome (SRX4011353).

Identification of conserved and novel miRNAs

Clean data were generated using the methodology detailed by Liu et al.[9]. sRNA within the size range of 18–30 nucleotides (nt) were extracted from the clean reads and subsequently aligned to the peach reference genome (www.rosaceae.org/organism/Prunus/persica) using Bowtie[31]. To exclude non-miRNA sequences, the Rfam (www.sanger.ac.uk/Software/Rfam) and GenBank (www.ncbi.nlm.nih.gov/GenBank) databases were used to filter out coding RNAs, rRNAs, tRNAs, small nuclear RNAs (snRNAs), and small nucleolar RNAs (snoRNAs). To identify conserved miRNAs, the small RNA reads were further mapped to the annotated miRNAs in miRBase 22. After removing the reads classified as conserved miRNAs, miREvo[32], and mirdeep2[33] with default parameters were integrated to predict novel miRNAs in the peach genome.

Differential expression analysis of miRNAs

Differentially expressed miRNAs were identified by calculating the transcripts per million (TPM) values for each miRNA as follows: (miRNA counts / total mapped reads) × 1,000,000. Differential expression analyses of DPA50 vs DPA20 and DPA75 vs DPA50 were then performed using the DEGseq (2010) *R* package. *P*-values were adjusted as described previously using q-value < 0.01 and |log2(foldchange)| > 1 as the thresholds for significant differential expression[34].

Analysis of degradome sequencing data

Raw sequencing reads were processed using the Illumina software to remove adaptors and low-quality reads. The extracted sequencing reads were subsequently analyzed using the Cleave Land pipeline to identify potentially miRNA-mediated cleavage targets[35]. Degradome reads were aligned to the mRNA sequences obtained from the Genome Database for Rosaceae (GDR) (www.rosaceae.org/species/prunus_persica/genome_v1.0), with only perfectly matching alignment(s) for degradation analysis. All reads were reverse-complemented and mapped to the miRNAs identified in this study, allowing a maximum of four mismatches. Alignments were retained and scored if the degradome sequence position corresponded to the 10th or 11th nucleotide of the miRNA. Targets were selected and categorized into classes 0, 1, 2, 3, or 4 as previously described[22]. In addition, to analyse miRNA targets and RNA degradation patterns, t-plots were built according to the distributions of signatures (and abundances) of transcripts. All identified targets were subjected to BlastX analysis to assess sequence similarities, followed by gene ontology (GO) analysis (www.geneontology.org) to elucidate miRNA regulatory networks. Network visualization and analysis were performed using the Cytoscape platform[36].

Validation of miRNA and target gene expression using quantitative Reverse Transcriptase Polymerase Chain Reaction (qRT-PCR)

To validate the sequencing results, the expression levels of five miRNAs and nine target genes were confirmed using qRT-PCR. cDNA synthesis was performed following the method described by Zhang et al.[19]. The precise sequence of ppe-miRNA was used as the forward primer and the miR-RACE 3'-primer was used as the reverse primer (Supplementary Table S1)[37]. Gene-specific primers overlapping with predicted complementary sites were designed for target gene amplification (Supplementary Table S1). qRT-PCR was conducted on a Rotor-Gene 3000 instrument (Corbett Robotics, Australia) using Rotor-Gene software version 6.1[38] and SYBR Green reaction mix (Toyobo, Osaka, Japan). U6 and RPII were used as internal controls for miRNA and mRNA normalization, respectively[39]. Each sample was analyzed with three biological replicates and three technical replicates to ensure reproducibility and reliability.

RNA ligase-mediated 5' RACE

RLM-5'RACE was performed using the SMARTer™ RACE cDNA Amplification Kit (Clontech Laboratories Inc., PaloAlto, CA, USA) following the manufacturer's instructions. Briefly, the RNA adapter was ligated to the purified RNAs as described by Zhang et al.[19]. The ligation products were then reverse transcribed, followed by PCR amplification using universal primers and gene-specific primers (Supplementary Table S1). The RACE products were gel-purified, cloned, and sequenced for further analysis.

Results

Identification of three key sampling points for double-sigmoid growth patterns of peach development

Growing peaches display typical double-sigmoid growth patterns, but the key transition points of peach vary across peach varieties. Therefore, to elucidate the regulatory mechanisms underlying peach development, it is essential to conduct analyses at multiple time points. To address this, we collected fruit samples from

10-year-old 'Baifeng' peach trees at various stages post-flowering (Fig. 1), and measured the longitudinal and transverse diameters of the fruits.

Our observations confirmed the double-sigmoid growth pattern in 'Baifeng' peach fruits (Supplementary Fig. S1). From 10 to 40 d post-anthesis (DPA10 to DPA40), the fruits underwent the first exponential growth phase (FWI). This was followed by a slow growth phase (FWII) from DPA40 to DPA63, characterized by hardening of the fruit core. Subsequently, from DPA63 to DPA87, the fruits entered a second exponential growth phase (FWIII). Based on these findings, we selected DPA20, DPA50, and DPA75 as representative time points for FWI, FWII, and FWIII, respectively.

Global analysis of sequences from small RNA and degradome libraries

To identify miRNAs involved in the development of peach fruit, three sRNA libraries representing DPA20, DPA50, and DPA75 were constructed and sequenced. In total of 12,017,340, 12,258,319, and 10,356,759 raw reads were generated from the DPA20, DPA50, and DPA75 libraries, respectively (Supplementary Table S2). After filtering out low-quality reads, adapters, junk reads, and redundant repeats, 11,429,372, 11,828,096, and 9,995,951 clean reads were obtained. Small RNAs ranging from 18 to 30 nucleotides (nt) accounted for 85.05% (DPA20), 89.79% (DPA50), and 93.64% (DPA75) of the clean reads (Supplementary Table S2) and were retained for further analysis. The length distribution of sRNAs was analyzed across the three libraries (Fig. 2). sRNAs with 21 and 24 nt were the most abundant, collectively representing an average of 75.5% of all sRNAs. However, the length distribution varied slightly among libraries: 21-nt sRNAs constituted 29.4% of the reads in the DPA75 library, while 24-nt sRNAs were predominant in the DPA20 and DPA50 libraries, accounting for 18.3% and 22.8% of the reads, respectively.

To identify miRNA targets during peach fruit development, transcriptome-wide degradome sequencing was performed to detect miRNA-mediated cleavage sites, which are characterized by endonucleolytic cleavage driven by extensive, often perfect, mRNA complementarity[40]. These analyses identified 26,557,773, 24,876,000, and 31,586,572 raw reads from the DPA20, DPA50, and DPA75 libraries, respectively (Supplementary Table S2). Approximately 7.27, 6.88, and 7.69 million unique sequences were successfully mapped to the peach genome sequences, accounting for 99.29% of all unique reads (Supplementary Table S2). Among these, over 60% of the reads were mapped to peach cDNA sequences, and all mapped sequences were subsequently used to identify miRNA targets.

Identification and characterization of known and novel miRNAs in peach fruit

To identify fruit-specific miRNAs, mRNA sequences from DPA20, DPA50, and DPA75 fruits were aligned with known miRNAs from the publicly available database miRbase (version 22). Following a series of screening, 124 known miRNAs belonging to 75 families and 86 novel miRNAs were identified in the three peach fruit samples (Table 1; Supplementary Table S3). We further analyzed the distribution of these miRNAs among the three stages. Among the known miRNAs, 85 (68.5%) were detected in all stages, while seven miRNAs (ppe-miR5225-3p, ppe-miR5225-5p, ppe-miR6267a, ppe-miR6280, ppe-miR6282, ppe-miR6283, and ppe-miR8127-5p) were exclusively detected in DPA20 fruits, four (ppe-miR169f, ppe-miR6266a, ppe-miR6285, and ppe-miR8130-5p) were specific to DPA50 and 13 (ppe-miR156f, ppe-miR2111a, ppe-miR319b, ppe-miR6260, ppe-miR6261, ppe-miR6263, ppe-miR6271, ppe-miR6287, ppe-miR6288b-3p, ppe-miR6290, ppe-miR6292, ppe-miR6297b, and ppe-miR8128-5p) were unique to DPA75 (Fig. 3 & Table 1).

These stage-specific miRNAs are likely to play regulatory roles during peach fruit development. Notably, expression levels of some members within known miRNA families varied significantly across growth stages. For example, eight members of the ppe-miR482 family were detected, while only one miRNA was identified for each of the other 41 families (Table 1).

Among 86 novel miRNA sequences, 79 were detected in all three development stages, whereas one (novel_193) was specific to DPA50 fruit, and five (novel_100, novel_101, novel_197, novel_59, and novel_99) were detected in DPA50 and DPA75 fruits but not in DPA20. The characteristics of all 86 novel miRNAs are summarized in Supplementary Table S3. The lengths of these novel miRNAs varied from 20 to 25 nt, with the majority (64.0%) being 24 nt in length (64.0%). The precursor lengths varied from 52 to 293 nt, with an average minimum free energy (MFE) of −71.70 kCal/mol. Nucleotide bias analysis revealed that novel miRNAs with a uridine (U) residue at their 5' end were the most frequent (54.17%) among 20 to 25-nt miRNAs (Supplementary Fig. S2)[41].

Spatiotemporal expression patterns of miRNAs during peach development

The abundance of miRNA reads in a library reflects the relative expression levels of miRNAs. In this study, the transcripts per million

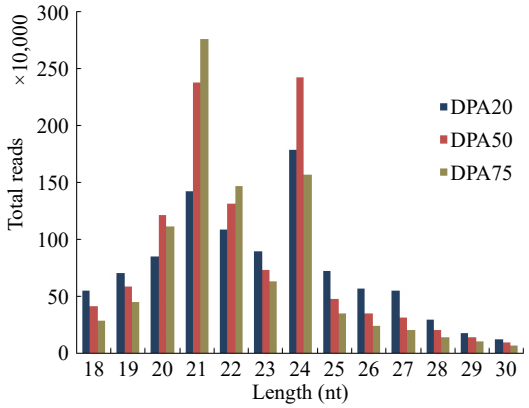

Fig. 2 Length distributions of sRNAs of peaches in the libraries at 20 d post anthesis (DPA20), DPA50, and DPA75.

Fig. 1 Fruit profiles at defined peach developmental stages (scale bar = 1 cm).

Table 1. Characteristics of know miRNAs identified from DPA20, DAP50, and DPA75 libraries in peach fruit.

miRNA ID	miRNA sequences (5'-3')	LT[1]	TPM[2]		
			DPA20	DPA50	DPA75
ppe-miR1511-5p	CGUGGUAUCAGAGUCAUGUUA	21	154,692.1383	14,578.83618	17,587.11608
ppe-miR1511-3p	ACCUGGCUCUGAUACCAUAAC	21	21.90796464	20.71184303	44.79237715
ppe-miR156a	UGACAGAAGAAAGAGAGCAC	20	0	4.602631785	26.46822286
ppe-miR156c	UGACAGAAGAGAGUGAGCAC	20	0	16.10921125	22.39618858
ppe-miR156f	UGACAGAAGAUAGAGAGCAC	20	0	0	10.18008572
ppe-miR159a	UUUGGAUUGAAGGGAGCUCUA	21	217,885.6623	131,131.2809	98,590.05813
ppe-miR159b	CUUGGAUUGAAGGGAGCUCCA	21	381,669.606	15,059.8112	12,138.73421
ppe-miR160a	UGCCUGGCUCCCUGUAUGCCA	21	1,084.44425	333.6908044	177.1334915
ppe-miR162	UCGAUAAACCUCUGCAUCCAG	21	9,792.860194	7,748.53061	4,200.303367
ppe-miR164a	UGGAGAAGCAGGGCACGUGCA	21	613.4230099	2,285.206681	804.2267716
ppe-miR164d	UGGAGAAGCAGGGCACAUGCU	21	10.95398232	2.301315892	0
ppe-miR166a	UCGGACCAGGCUUCAUUCCCC	21	18,358.87437	7,847.487193	3,273.915566
ppe-miR167a	UGAAGCUGCCAGCAUGAUCUA	21	1,424.017702	352.1013315	677.9937087
ppe-miR167c	UGAAGCUGCCAGCAUGAUCUGA	22	3,768.169918	844.5829325	659.6695544
ppe-miR167d	UGAAGCUGCCAGCAUGAUCUUA	22	1,577.373454	342.896068	494.7521658
ppe-miR168	UCGCUUGGUGCAGGUCGGGAA	21	492.9292044	92.0526357	89.5847543
ppe-miR169f	UAGCCAAGGAUGACUUGCCUGC	22	0	2.301315892	0
ppe-miR171b	UUGAGCCGCGCCAAUAUCACU	21	120.4938055	23.01315892	30.54025715
ppe-miR171d-5p	UGUGAUAUUGGUUCGGUUCAUA	22	10.95398232	11.50657946	22.39618858
ppe-miR171d-3p	CGAGCCGAAUCAAUAUCACUC	21	10.95398232	4.602631785	16.28813715
ppe-miR171e	UUAUUGAACCGGACCAAUAUC	21	10.95398232	2.301315892	0
ppe-miR171f	UGAUUGAGCCGUGCCAAUAUC	21	295.7575226	133.4763218	67.18856573
ppe-miR171h	UUGAGCCGCGUCAAUAUCUCC	21	635.3309746	211.7210621	24.43220572
ppe-miR172a-3p	AGAAUCUUGAUGAUGCUGCAU	21	120.4938055	20.71184303	12.21610286
ppe-miR172c	GGAAUCUUGAUGAUGCUGCAU	21	32.86194696	4.602631785	16.28813715
ppe-miR172d	GGAAUCUUGAUGAUGCUGCAG	21	65.72389392	2.301315892	4.072034287
ppe-miR2111a	UAAUCUGCAUCCUGAGGUUUA	21	0	0	2.036017143
ppe-miR319a	UUGGACUGAAGGGAGCUCCC	20	164.3097348	29.9171066	171.02544
ppe-miR319b	UAGCUGCCGAGUCAUUCAUCCA	22	0	0	2.036017143
ppe-miR319c	UUUGGACUGAAGGGAGCUCC	20	54.7699116	29.9171066	24.43220572
ppe-miR319d	CUUGGACUGAAGGGAGCUCCC	21	251.9415934	20.71184303	16.28813715
ppe-miR319e	CUUGGACUGAAGGGAGCUCCU	21	328.6194696	36.82105428	81.44068573
ppe-miR319f	UUUGGACUGAAGGGAGCUCUC	21	109.5398232	126.5723741	77.36865144
ppe-miR3627-5p	UCGCAGGAGAGAUGGCACUGUC	22	43.81592928	6.903947677	2.036017143
ppe-miR390	AAGCUCAGGAGGGAUAGCGCC	21	153.3557525	2.301315892	0
ppe-miR393a	CAUCCAAAGGGAUCGCAUUGA	21	262.8955757	87.45000391	136.4131486
ppe-miR393b	UCCAAAGGGAUCGCAUUGAUC	21	306.711505	128.87369	215.8178172
ppe-miR394a	UUGGCAUUCUGUCCACCUCC	20	3,308.102661	3,516.410684	3,249.483361
ppe-miR394b	UUGGCAUUCUGUCCACCUCC	20	54.7699116	39.12237017	44.79237715
ppe-miR395a-3p	CUGAAGUGUUUGGGGGGACCC	21	898.2265503	2,908.863288	1,667.49804
ppe-miR395c	CUGAAGUGUUUGGGGGAACUC	21	65.72389392	174.9000078	215.8178172
ppe-miR396a	UUCCACAGCUUUCUUGAACGU	21	6,364.263728	59,399.2645	71,602.65089
ppe-miR396b	UUCCACAGCUUUCUUGAACUU	21	61,791.41427	484,650.223	540,299.9053
ppe-miR396c	UUCCACAGCUUUCUUGAACUG	21	12,421.81595	118,018.3829	109,040.9341
ppe-miR397	UCAUUGAGUGCAGCGUUGAUG	21	43.81592928	85.14868802	46.8283943
ppe-miR398a-5p	GGAGCGACCUGGGAUCACAUG	21	6,484.757534	11,021.00181	2,640.714235
ppe-miR398a-3p	UGUGUUCUCAGGUCGCCCCUG	21	109.5398232	71.34079267	59.04449715
ppe-miR398b	CGUGUUCUCAGGUCGCCCCUG	21	1,654.05133	35,502.40027	37,275.40186
ppe-miR398c	UGUGUUCUCAGGUCACCCCUU	21	32.86194696	55.23158142	22.39618858
ppe-miR399a	CGCCAAAGGAGAGUUGCCCUU	21	0	34.51973839	114.01696
ppe-miR399b	UCUGCCAAAGGAGAAUUGCCC	21	32.86194696	27.61579071	73.29661716
ppe-miR399c	UGCCAAAGAAGAGUUGCCCUA	21	0	11.50657946	8.144068573
ppe-miR403	UUAGAUUCACGCACAAACUCG	21	230.0336287	191.0092191	425.5275829
ppe-miR477-5p	ACUCUCCCUCAAAGGCUUCUAG	22	0	6.903947677	8.144068573
ppe-miR477-3p	CGAAGCCUUUGGGGAGAGUAA	21	87.63185856	561.5210778	486.6080972
ppe-miR477a-3p	GUUGGGGGCUCUUUUGGGACG	21	65.72389392	987.2645179	787.9386344
ppe-miR477a-5p	UCCCUCAAGGGCUCCCAAUAUU	22	0	64.43684499	103.8368743
ppe-miR482a-3p	UUUCCGAAACCUCCCAUUCCAA	22	3,833.893812	697.2987154	238.2140058
ppe-miR482a-5p	GGGUGAGAGGUUGCCGGAAAGA	22	449.1132751	98.95658337	42.75636001
ppe-miR482b-5p	GGAAUGGGAGGAUUGGGAAAA	21	12,750.43542	3,960.564651	2,972.585029
ppe-miR482b-3p	CUUCCCAAACCUCCCAUUCCUA	22	32.86194696	4.602631785	10.18008572
ppe-miR482c-5p	GGAAUGGGCUGUUUGGGAUG	20	755.8247801	409.6342289	191.3856115
ppe-miR482c-3p	UUCCCAAGCCCGCCCAUUCCAA	22	3,428.596466	554.6171301	555.8326801

(to be continued)

Table 1. (continued)

miRNA ID	miRNA sequences (5'-3')	LT[1]	TPM[2]		
			DPA20	DPA50	DPA75
ppe-miR482e	UUGCCUAUUCCUCCCAUGCCAA	22	942.0424795	849.1855643	572.1208173
ppe-miR482f	UCUUUCCUACUCCACCCAUUCC	22	8,839.863732	10,813.88338	16,467.30665
ppe-miR5225-3p	UCAUCUCUCCUCGACUGAA	19	21.90796464	0	0
ppe-miR5225-5p	UCUGUCGUAGGAGAGAUGGCGC	22	32.86194696	0	0
ppe-miR530	UCUGCAUUUGCACCUGCACCU	21	87.63185856	23.01315892	30.54025715
ppe-miR535a	UGACAACGAGAGAGAGCACGC	21	76.67787624	62.1355291	12.21610286
ppe-miR535b	UGACGACGAGAGAGAGCACGC	21	197.1716818	186.4065873	77.36865144
ppe-miR6257	UCUUAACUGUUGGAUUAGGCU	21	10.95398232	11.50657946	2.036017143
ppe-miR6258	UUCCAGCUGUAAAGAUCAAGA	21	10.95398232	6.903947677	12.21610286
ppe-miR6260	UGGAGUGAGAGAAUGGGAGGU	21	0	0	6.10805143
ppe-miR6261	AAGUGAUUAUAUGGAGAAGCAC	22	0	0	2.036017143
ppe-miR6263	AAGUGGACAAAAGGGGAGUGG	21	0	0	2.036017143
ppe-miR6264	AUGCCUAUGGACACGUGUCAA	21	10.95398232	4.602631785	6.10805143
ppe-miR6265	UUGAACUUUGACCCGAUUCGCAU	23	21.90796464	4.602631785	2.036017143
ppe-miR6266a	UAAAUGCAGGGGCAAAAUGAU	21	0	2.301315892	0
ppe-miR6267a	UAGAGAGGUGGUACAAUUGUG	21	10.95398232	0	0
ppe-miR6267c-5p	AUUGCUGAUCACCUCUCUAAU	21	21.90796464	59.8342132	185.27756
ppe-miR6267c-3p	UAGAGAGAUGGUCAGCAAUGU	21	21.90796464	27.61579071	105.8728914
ppe-miR6270	UUCUGGUAUUGGAAUUUCAUU	21	142.4017702	18.41052714	40.72034287
ppe-miR6271	UCAAGAUUGAGAGAUAUAAUG	21	0	0	8.144068573
ppe-miR6274b-5p	AUUUCGACUAAUAACACAAUG	21	0	2.301315892	2.036017143
ppe-miR6274b-3p	UUGUGUUAUUGGCCGAAAAUAG	22	208.1256641	18.41052714	46.8283943
ppe-miR6277	UGUGUGUGGAAAGAGCGAGAC	21	21.90796464	9.20526357	12.21610286
ppe-miR6280	UUGGCAGUAAGAUUUUUGGUG	21	10.95398232	0	0
ppe-miR6281	GUUAGAGAUAGAGAGAGUGAG	21	76.67787624	52.93026553	69.22458287
ppe-miR6282	GUUGAUCGAUGUGGGAUGUUACA	23	10.95398232	0	0
ppe-miR6283	CAAAAGGGGAGUGGGAAAAUC	21	21.90796464	0	0
ppe-miR6284	UUUGGACCAUGGAUGAAGAUU	21	98.58584088	29.9171066	20.36017143
ppe-miR6285	UAGUGAAGUUUGAAUUAGGGCU	22	0	2.301315892	0
ppe-miR6287	CAAGAAGUGGAAGUUUUGGGC	21	0	0	2.036017143
ppe-miR6288a	GAAAAUGACAAGUGGCUAGUU	21	0	2.301315892	2.036017143
ppe-miR6288b-3p	UCAAUUAGAAAAUGAUAAGUG	21	0	0	4.072034287
ppe-miR6290	UGAAUGAGUUCAGAGAUCGUGUA	23	0	0	2.036017143
ppe-miR6292	UAUCUUUUAAUCGUUAGAUCA	21	0	0	2.036017143
ppe-miR6293	UAAGAGGCUGAUGACUAAAAC	21	65.72389392	46.02631785	61.0805143
ppe-miR6294	UGGUGUAGGCUAAUCACAAUC	21	32.86194696	20.71184303	42.75636001
ppe-miR6295	GAGGACAGAAGAUGAUUCAGC	21	32.86194696	13.80789535	20.36017143
ppe-miR6297a	AAUAAUUUUUCGUCGCGCAAAAU	23	32.86194696	20.71184303	8.144068573
ppe-miR6297b	GAUGUAUUGUCGUCGCGCAAAGU	23	0	0	2.036017143
ppe-miR7122a-5p	UUAUACAAUGAAAUCACGGCCG	22	251.9415934	69.03947677	83.47670287
ppe-miR7122a-3p	GCCGUGUUUCUUUGUAUAAAG	21	1,237.800002	1,456.73296	2,158.178172
ppe-miR7122b-3p	CCGUGUUUCCUUGUAUAAAG	20	0	2.301315892	8.144068573
ppe-miR7122b-5p	UUAUACAAUGAAAUCACGGUCG	22	32.86194696	46.02631785	140.4851829
ppe-miR7125-3p	CGAACUUAUUGCAACUAGCUU	21	0	27.61579071	8.144068573
ppe-miR8122-5p	UUCCACAGAUCUUUCCUCAUU	21	5,466.037178	1,233.505318	1,284.726817
ppe-miR8122-3p	UGAAGGAAGAUUUGUGGAAAG	21	887.2725679	667.3816088	637.2733658
ppe-miR8124-3p	UGGCACCAAUGAUACCAAGUUU	22	54.7699116	11.50657946	4.072034287
ppe-miR8124-5p	ACUUGGUAUCUUGGUGCCGGU	21	0	2.301315892	2.036017143
ppe-miR8125	CAGGAAAGAAUGUGAUGAGUA	21	65.72389392	27.61579071	46.8283943
ppe-miR8126-5p	UCUGAGUCAGAUUACUGAAUA	21	10.95398232	4.602631785	8.144068573
ppe-miR8126-3p	UUCAGUAUUUUGACUCAGAA	20	21.90796464	23.01315892	42.75636001
ppe-miR8127-3p	UUCAAAGGGUACAUCCACAGU	21	10.95398232	0	0
ppe-miR8128-5p	AUUAGACCUCUCCCGACGAAA	21	21.90796464	43.72500196	63.11653144
ppe-miR8128-3p	UCGUGGGGAGAGAUCUAAUCG	21	0	0	4.072034287
ppe-miR8130-5p	GGGUUCCUUGUUGGAAGGACU	21	0	2.301315892	0
ppe-miR8131-5p	AUUUCAGCUAAGUUGAGUUGU	21	10.95398232	0	2.036017143
ppe-miR8132	UCCAACGAUGGGUGACCACAA	21	10.95398232	2.301315892	10.18008572
ppe-miR8133-5p	UCCUGUGCGAACGUCCAGAAG	21	87.63185856	46.02631785	28.50424001
ppe-miR8133-3p	UAACUUCCGAACGUCCGCAUA	21	32.86194696	16.10921125	12.21610286
ppe-miR827	UUAGAUGACCAUCAACAAACA	21	1,084.44425	409.6342289	309.4746058
ppe-miR858	CUCGUUGUCUGUUCGACCUUG	21	10.95398232	4.602631785	2.036017143

[1] Length of miRNA; [2] the expression of transcripts per million.

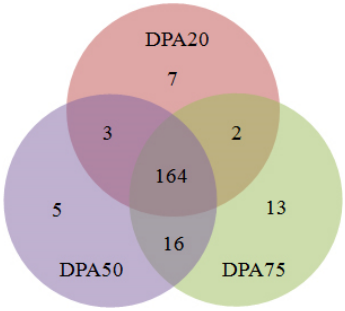

Fig. 3 Venn diagram of peach miRNAs among these libraries at DPA20, DPA50, and DPA75.

(TPM) values of known and novel miRNAs ranged from 0 to 381,669.61 (ppe-miR159b) in DPA20, 0 to 484,650.22 (ppe-miR396b) in DPA50, and 0 to 540,299.90 (ppe-miR396b) in DPA75. The expression patterns of miRNAs varied widely, with TPM values spanning several orders of magnitude (Table 1; Supplementary Table S3). Among the novel miRNAs, novel_128 and novel_132 exhibited significantly higher expression levels compared to others, suggesting their potential importance in peach fruit development. Specifically, novel_128 showed the highest read counts in DPA75, while novel_132 was most abundant in DPA20. These findings indicate that novel_128 may play a critical role during the FWIII stage, whereas novel_132 is likely more important during the FWI stage. Among the known miRNAs, ppe-miR159b had the highest number of sequenced reads in DPA20, while ppe-miR396b dominated in DPA50 and DPA75, suggesting stage-specific regulatory roles for these miRNAs in peach development.

To further elucidate the roles of miRNAs during fruit development, we analyzed their abundance patterns across the three stages. As shown in Supplementary Fig. S3, 210 miRNAs were categorized into four groups based on their accumulation trends. Some miRNAs, such as ppe-miR156a, ppe-miR156c, ppe-miR399a, ppe-miR395c, and ppe-miR398b, exhibited sustained increases across all three stages. In contrast, others, including ppe-miR160a, ppe-miR164d, ppe-miR166a, and ppe-miR171f, showed sustained decreases (Supplementary Fig. S3). Notably, different members of the same miRNA family displayed opposing expression trends. For example, ppe-miR164a expression increased by 3.7-fold at DPA50, while ppe-miR164d decreased by 4.7-fold compared to DPA20 levels. These observations highlight the functional diversity of miRNAs, even within the same family, during fruit development.

To investigate the roles of miRNAs in peach fruit development, we performed differential expression analyses between adjacent stages (DPA50 vs DPA20 and DPA75 vs DPA50). MiRNAs were considered differentially expressed if |log2(fold change)| w >1 and the associated *q*-value was < 0.01. In the DPA50 vs DPA20 comparison, 97 miRNAs were differentially expressed, with 39 up-regulated and 58 down-regulated (Supplementary Table S3). Similarly, in the DPA75 vs DPA50 comparison, 79 miRNAs showed differential expression, with 43 up-regulated and 36 down-regulated (Supplementary Table S4). These results suggest that up-regulated miRNAs may positively correlate with fruit development, while down-regulated miRNAs may have negative regulatory roles.

Identification of miRNA target genes using degradome sequencing

MiRNAs can regulate multiple target genes, and conversely, a single gene can be regulated by multiple miRNAs[42]. Therefore, identifying miRNA targets is crucial for understanding their functional roles. In this study, we performed genome-wide degradome sequencing to identify miRNA-guided RNA cleavage targets. A total of 216 sliced target genes were identified for 74 known and eight novel miRNAs across the three libraries using the Cleave Land pipeline (Supplementary Tables S5). Specifically, 120, 139, and 157 target mRNAs were cleaved in the DPA20, DPA50, and DPA75 libraries, respectively. Based on the heights of the degradome peaks at each occupied transcript position, these cleaved targets were classified into the categories 0, 1, 2, 3, and 4 (Supplementary Table S5)[43]. Analysis of the cleavage products revealed that target genes regulated by single miRNAs exhibited varying expression levels across the three developmental stages, as illustrated in Fig. 4. Additionally, the cleavage frequencies of target genes varied significantly during different stages of peach development.

Among all target mRNAs which are cleaved by miRNAs, three MYB domain protein 30 were found to be the targets of ppe-miR159a, but not all the corresponding cleavage products were found at the three developmental stages (Supplementary Table S5). Notably, the cleavage products of Prupe.2G050100_v2.0. a1(*GAM1*) are present at all stages in greater abundance than Prupe.3G216600_v2.0.a1 (*GAM1*) and Prupe.4G215500_v2.0.a1(*GAM1*) (Fig. 4; Supplementary Table S5). These observations differ from the findings of previous reports which failed to detect the cleavage products of the miR159a[44], likely reflecting different species and developmental stages. The miR160 family is known to target transcription factor genes of the ARF family, which are involved in the auxin signaling pathway during plant development[45]. Four *ARF* genes with cleavage products were detected across all three developmental stages, including Prupe.1G507000_v2.0.a1, which has been previously validated[44]. For ppe-miR167a, a different ARF family member (Prupe.3G011800_v2.0. a1) was identified as a target (Supplementary Table S5; Fig. 5), suggesting that ppe-miR167a also involved in auxin signaling during peach development.

In tomatoes, *TIR1* and two *TIR1* homologs have been identified as targets of miR393 family[41]. Here we found that *TIR1* (Prupe.8G253300_v2.0.a1) and *AFB2* (Prupe.3G311800_v2.0.a1) are targeted by ppe-miR393a and ppe-miR393b. However, the cleavage products of ppe-miR393b target genes were significantly more abundant, while no cleavage products of *AFB2* (Prupe.3G311800_v2.0.a1) were detected for ppe-miR393a. These results suggest that ppe-miR393b plays a critical role in peach development, particularly during the FWI stage, with peak degradation occurring around 20 DPA, consistent with findings in tomatoes[42]. Additionally, two MYB domain protein genes were identified as targets of ppe-miR159b, similar to ppe-miR159a. Both miRNAs were found to cleave Prupe.2G050100_v2.0.a1 (*GAM1*) and Prupe.4G215500_v2.0.a1 (*GAM1*), confirming that a single miRNA can regulate multiple genes and that multiple miRNAs can collectively regulate a single gene[42].

GO pathway analysis and identification of fruit development-specific miRNA-mediated regulatory networks

We identified 216 target genes through degradome sequencing and performed Gene Ontology (GO) pathway analyses to elucidate their functional roles. Differentially expressed target genes in the DPA50 vs DPA20 comparison were classified into 382 GO terms, with 25 significantly enriched terms (p-value ≤ 0.05), including 13 biological processes, eight molecular functions, and four cellular components (Supplementary Table S6). Key enriched biological processes included cell differentiation (GO:0030154), auxin-activated signaling (GO:0009734), and leaf development (GO:0048366). In the cellular component category, the nucleus (GO:0005634), microtubule (GO:0005874), and endosome (GO:0005768) were predominant, while ADP binding (GO:0043531), ATP binding (GO:0005524),

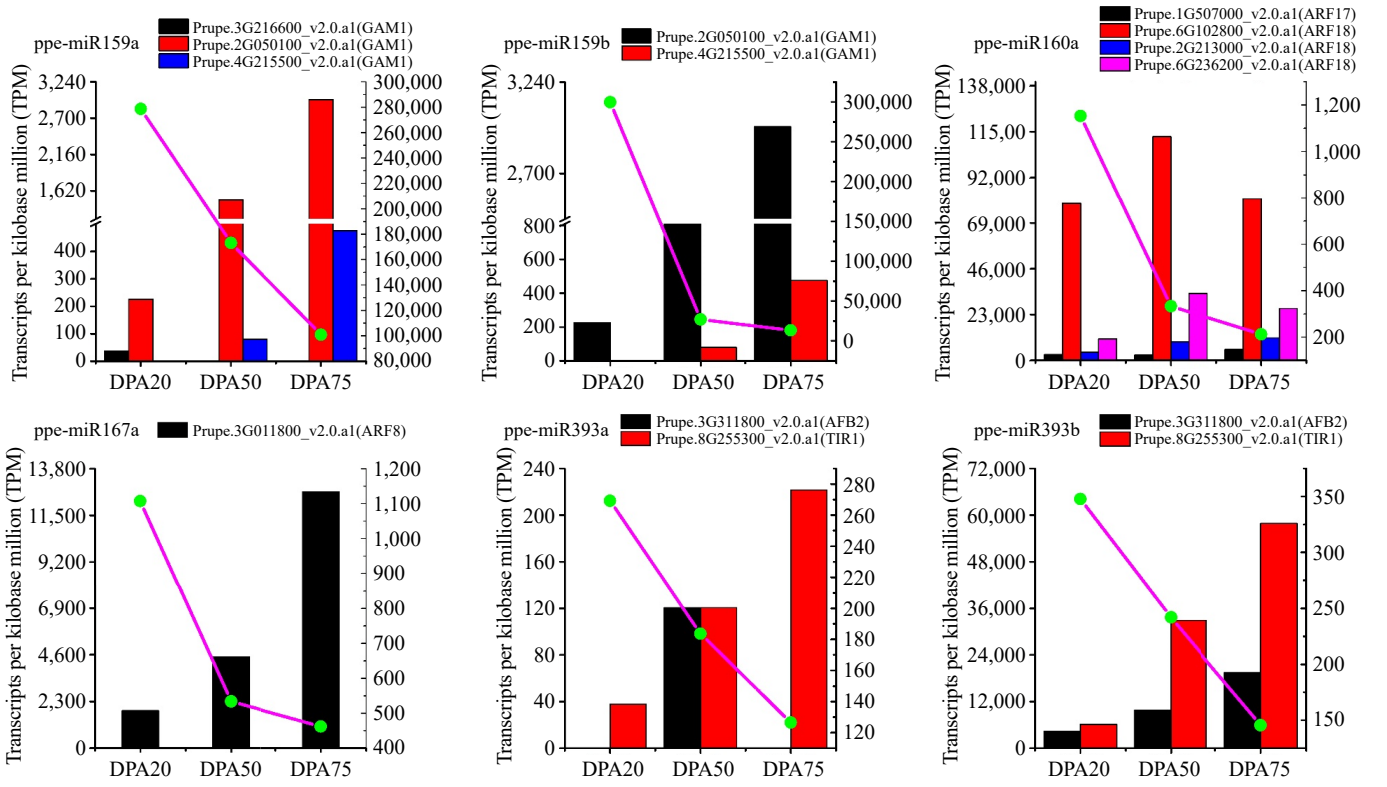

Fig. 4 Abundance of miRNA and its target genes at different peach developmental stages. Normalized sequenced read abundance, height = transcripts per kilobase million reads (TPM) on the y-axis. The histogram represents the abundance of miRNA target genes and the dot linked by a line represent the abundance of miRNA.

and metal ion binding (GO:0046872) were highly enriched in the molecular function category (Supplementary Table S6). The top 20 enriched GO terms for the DPA50 vs DPA20 comparison are illustrated in Supplementary Fig. S4a. Similarly, in the DPA75 vs DPA50 comparison, differentially expressed target genes were classified into 391 GO terms, with 27 significantly enriched terms (p-value ≤ 0.05), including 15 biological processes, nine molecular functions, and three cellular components (Supplementary Table S6). Key biological processes included transcription (GO:0006351), cell differentiation (GO:0030154), and auxin-activated signaling (GO:0009734). The cellular component category was dominated by the nucleus (GO:0005634), cytosol (GO:0005829), and extracellular region (GO:0005576), while ADP binding (GO:0043531), metal ion binding (GO:0046872), and DNA binding (GO:0003677) were highly enriched in the molecular function category (Supplementary Table S6). The top 20 enriched GO terms for the DPA75 vs DPA50 comparison are shown in Supplementary Fig. S4b. These results suggest that the targets of some miRNAs that were identified by degradome sequencing are involved in many biological processes during peach development.

Our GO analyses revealed that the most enriched target mRNAs are associated with cell differentiation (GO:0030154) and auxin-activated signaling (GO:0009734), both of which are critical for peach fruit development. Congruently, fruit development is accompanied by constant division and differentiation of cells, and a previous report showed concordant effects of auxin on fruit enlargement[46]. To investigate the relationships among cell differentiation, auxin-activated signaling, ppe-miRNAs, and their targets, we conducted network analyses using the Cytoscape platform. This analysis included 23 miRNAs and 26 target genes known to be involved in cell differentiation, cell division, auxin transport, and auxin signaling (Table 2 & Fig. 5). The network revealed that a single pathway can be regulated by multiple miRNAs, and a single miRNA can influence multiple pathways, such as the auxin-activated signaling pathway. Specifically, we identified six ppe-miRNAs (ppe-miR160a, ppe-miR164a, ppe-miR164d, ppe-miR167a, ppe-miR393a, and ppe-miR393b) targeting 11 mRNAs, including auxin response factors, auxin receptor mRNAs, and NAC domain transcriptional regulators. For example, ppe-miR164d targets Prupe.4G143600_v2.0.a1 and Prupe.1G413900_v2.0.a1, both of which are involved in auxin signaling and cell differentiation. Similarly, ppe-miR160a targets Prupe.2G213000_v2.0.a1, Prupe.6G102800_v2.0.a1, and Prupe.6G236200_v2.0.a1, which are associated with auxin-activated signaling and cell division (Table 2 & Fig. 5). These findings demonstrate that a complex miRNA-mediated regulatory network governs multiple biological processes during peach development.

Validation of identified miRNAs and their targets in peach

To validate the deep sequencing data, we employed the RLM-5'RACE approach to confirm four targets of ppe-miR160a and two targets of ppe-miR393a/b. Additionally, the expression levels of five miRNAs and their corresponding target genes were analyzed using qRT-PCR. For this validation, we selected five conserved miRNAs (ppe-miR159b, ppe-miR160a, ppe-miR167a, ppe-miR393a, and ppe-miR393b) and their target mRNAs, including auxin response factors, TIR proteins involved in auxin signaling, and MYB domain proteins. As shown in Fig. 6, five miRNAs showed differential expression patterns during fruit development. The expression levels of ppe-miR160a and ppe-miR159b gradually decreased throughout fruit development, while ppe-miR167a, ppe-miR393a, and ppe-miR393b showed an initial decline from DPA20 to DPA50, followed by an increase from DPA50 to DPA75 (Fig. 6). These expression patterns align with our high-throughput sequencing data (Table 1;

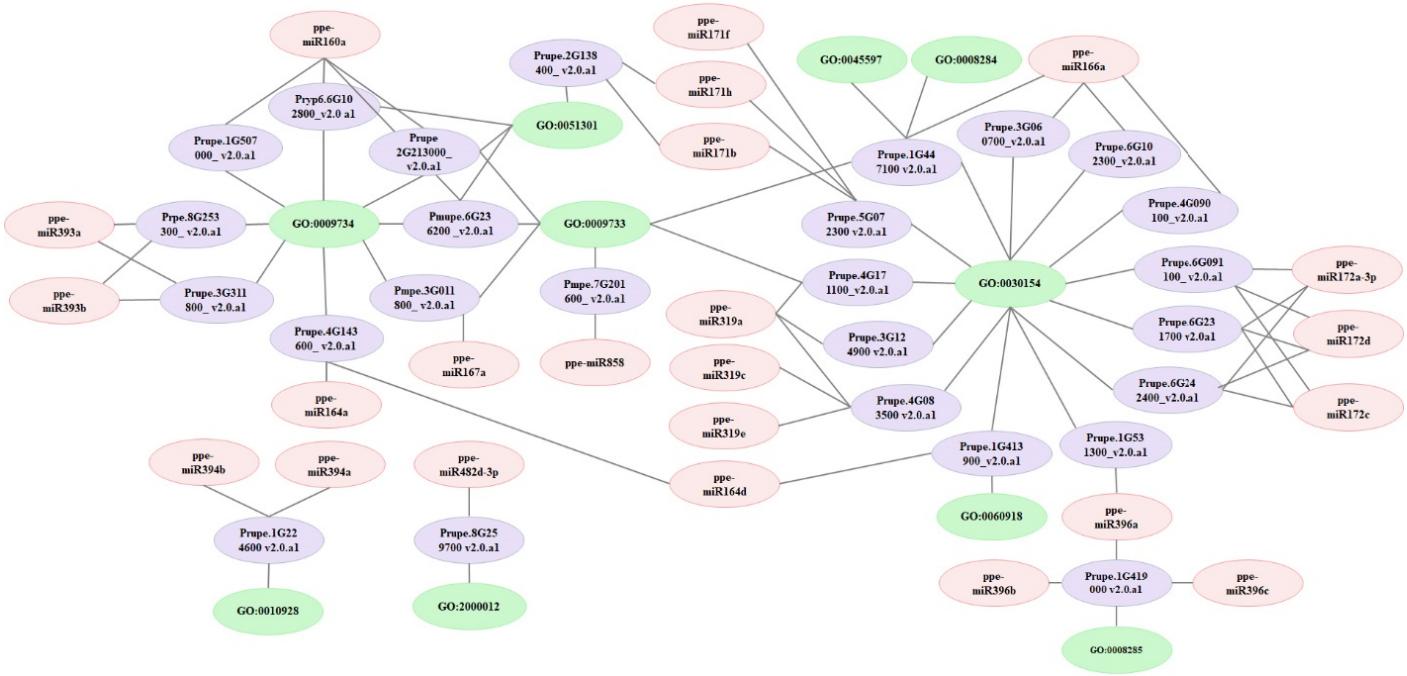

Fig. 5 Network analysis of miRNAs, targets, and GO terms involved in auxin signalling and fruit enlargement. Network analyses were performed using the Cytoscape network platform.

Supplementary Table S3) and are consistent with previous studies highlighting the critical roles of ppe-miR160, ppe-miR167, and ppe-miR393 in auxin signaling[44].

To further confirm the regulatory roles of these miRNAs, we examined the expression patterns of nine target genes corresponding to the five miRNAs using qRT-PCR at the same developmental stages (Fig. 6). As expected, the expression patterns of the miRNAs and their target genes exhibited an inverse relationship. This finding was supported by degradome sequencing data, which revealed abundant cleavage products for these target genes (Supplementary Table S5). Additionally, RLM-5'RACE results confirmed the same cleavage sites for four targets of ppe-miR160a and two targets of ppe-miR393b (Supplementary Fig. S5, Supplementary Tables S7 & S8), further validating the reliability of the degradome sequencing data.

Discussion

Numerous studies have highlighted the critical roles of miRNAs in fruit development[10,11,18,22,23]. Peach fruits are well-known to exhibit a double-sigmoid growth pattern, characterized by three distinct stages: FWI, FWII, and FWIII. While Zhu et al.[18] identified miRNAs in peach fruits using a mixed fruit sample, their analysis was limited to a single mixed library, leaving the dynamic regulation of miRNAs across sequential developmental stages largely unexplored. In this study, we conducted a comprehensive analysis of peach miRNAs and their targets across three key developmental stages, representing the double-sigmoid growth curve, through small RNA (sRNA) and degradome sequencing. Integrative analyses revealed that miRNA-mediated regulatory networks play a pivotal role in peach growth and development. However, the lack of biological replicates in our study presents a limitation in distinguishing true biological variations from technical noise. Future studies incorporating multiple replicates are essential to validate our findings and provide a more robust understanding of miRNA expression dynamics during peach fruit development.

MiRNAs during peach fruit development

Numerous fruit development-associated miRNAs have been identified in fruit-producing plants, including grape[16,17], apple[15], citrus[22], and peach[18]. In this study, 124 known miRNAs were detected across three small RNA libraries, with 85 miRNAs present in all three libraries. Previous studies have shown clear functional dose effects of miRNAs and suggested that highly and/or specifically expressed miRNAs are more likely to play versatile biological roles than with low abundance[47,48]. For example, in *Hami melon*, the miR159 and miR396 families exhibited high redundancy in their respective small RNA libraries[49]. Similarly, in our datasets, ppe-miR396b accounted for the highest proportion of normalized reads across all three libraries, representing approximately 50% of the known miRNA reads. In contrast, ppe-miR159a accounted for about 21% of conserved reads (Table 2), suggesting that both ppe-miR396b and ppe-miR159a play critical roles during peach development. Interestingly, in a mixed peach library from 'Troubadour', the ppe-miR156 family was the most abundantly expressed. However, in our study, ppe-miR156 was detected only in the DPA50 and DPA75 libraries, with no reads detected in the DPA20 library. This discrepancy suggests that single miRNAs may have distinct roles in different cultivars or developmental stages. Additionally, we identified 86 novel miRNAs, 79 of which were detected across all three libraries, while novel_193 was specific to the DPA50 library. The total number of novel miRNAs was lower than that of known miRNAs, and their absolute sequencing frequencies were considerably reduced, with most novel miRNAs exhibiting relatively low TPM values. This observation aligns with previous studies[50,51], which have shown that species-specific novel miRNAs often have low sequencing frequencies and exhibit more spatiotemporal expression patterns compared to conserved miRNAs.

Differences in miRNA expression profiles may reflect their regulatory roles in peach development. In this study, 97 and 79 miRNAs were differentially expressed in the DPA50 vs DPA20 and DPA75 vs DPA50 comparisons, respectively (Supplementary Table S4), indicating their involvement in cellular and developmental processes.

Table 2. The miRNA, target genes, and GO terms information used for network analysis.

GO_Id	GO_term	miRNA	DPA20_TPM	DPA50_TPM	DPA75_TPM	Transcript_ID	Symbol	Annoation	DPA20_TPM	DPA50_TPM	DPA75_TPM
GO:0009734	Auxin-activated signaling pathway	ppe-miR160a	1,084.44425	333.6908044	177.1334915	Prupe.1G507000_v2.0.a1	*ARF17*	Auxin response factor 3	2,936.993249	2,693.359061	5,571.987995
						Prupe.2G213000_v2.0.a1	*ARF18*	Auxin response factor 3	4,104.259796	9,286.058852	11,365.58915
						Prupe.6G102800_v2.0.a1	*ARF18*	Hypothetical protein	78,884.62636	112,477.8903	81,142.07518
						Prupe.6G236200_v2.0.a1	*ARF18*	Auxin response factor 3	10,806.629	33,566.48979	26,055.37568
		ppe-miR164a	613.4230099	2,285.206681	804.2267716	Prupe.4G143600_v2.0.a1	*NAC021*	NAC domain-containing protein 89-like	489.4988748	8,562.46985	5,160.4207
		ppe-miR164d	10.95398232	2.301315892	0	Prupe.4G143600_v2.0.a1	*NAC021*	NAC domain-containing protein 89-like	489.4988748	8,562.46985	5,160.4207
		ppe-miR167a	1,424.017702	352.1013315	677.9937087	Prupe.3G011800_v2.0.a1	*ARF8*	Auxin response factor 19-like	1,845.03422	4,502.331565	12,663.60908
		ppe-miR393a	262.8955757	87.45000391	136.4131486	Prupe.3G311800_v2.0.a1	*AFB2*	Protein TRANSPORT INHIBITOR RESPONSE 1-like	0	120.5981669	0
						Prupe.8G253300_v2.0.a1	*TIR1*	Hypothetical protein	37.6537596	120.5981669	221.6131589
		ppe-miR393b	306.711505	128.87369	215.8178172	Prupe.3G311800_v2.0.a1	*AFB2*	Protein TRANSPORT INHIBITOR RESPONSE 1-like	4,367.836113	9,848.850297	19,406.98092
						Prupe.8G253300_v2.0.a1	*TIR1*	Hypothetical protein	6,137.562814	32,923.29957	57,841.03448
GO:0010928	regulation of auxin mediated signaling pathway	ppe-miR394b	54.7699116	39.12237017	44.79237715	Prupe.1G224600_v2.0.a1	*FBX6*	–	978.9977495	4,140.537064	7,408.211312
		ppe-miR394a	3,308.102661	3,516.410684	3,249.483361	Prupe.1G224600_v2.0.a1	*FBX6*	–	978.9977495	4,140.537064	7,408.211312
GO:0009733	response to auxin	ppe-miR167a	1424.017702	352.1013315	677.9937087	Prupe.3G011800_v2.0.a1	*ARF8*	Auxin response factor 19-like	1,845.03422	4,502.331565	12,663.60908
		ppe-miR160a	1,084.44425	333.6908044	177.1334915	Prupe.2G213000_v2.0.a1	*ARF18*	Auxin response factor 3	4,104.259796	9,286.058852	11,365.58915
						Prupe.6G236200_v2.0.a1	*ARF18*	Auxin response factor 3	10,806.629	33,566.48979	26,055.37568
		ppe-miR858	10.95398232	4.602631785	2.036017143	Prupe.7G201600_v2.0.a1	*C1*	Transcription factor MYB75-like	0	40.19938897	886.4526356
		ppe-miR166a	18,358.87437	7,847.487193	3,273.915566	Prupe.1G447100_v2.0.a1	*ATHB-8*	–	414.1913556	2,170.767004	2,421.915237
		ppe-miR319a	164.3097348	29.9171066	171.02544	Prupe.4G171100_v2.0.a1	*PCF5*	–	112.9612788	0	94.9770681
GO:0060918	Auxin transport	ppe-miR164d	10.95398232	2.301315892	0	Prupe.1G413900_v2.0.a1	*SF21*	–	37.6537596	0	0
GO:2000012	Regulation of auxin polar transport	ppe-miR482d-3p	0	0	0	Prupe.8G259700_v2.0.a1	*OsI_027940*	Uncharacterized protein OsI_027940-like	37.6537596	120.5981669	31.6590227
GO:0030154	Cell differentiation	ppe-miR319c	54.7699116	29.9171066	24.43220572	Prupe.4G083500_v2.0.a1	*TCP2*	–	0	0	63.3180454
		ppe-miR319e	328.6194696	36.82105428	81.44068573	Prupe.4G083500_v2.0.a1	*TCP2*	–	0	0	63.3180454
		ppe-miR164d	10.95398232	2.301315892	0	Prupe.1G413900_v2.0.a1	*SF21*	–	37.6537596	0	0
		ppe-miR166a	18,358.87437	7,847.487193	3,273.915566	Prupe.1G447100_v2.0.a1	*ATHB-8*	–	414.1913556	2,170.767004	2,421.915237
						Prupe.3G060700_v2.0.a1	*ATHB-15*	–	414.1913556	2,170.767004	2,421.915237
						Prupe.4G090100_v2.0.a1	*ATHB-14*	–	941.3439899	924.5859463	569.8624086
						Prupe.6G102300_v2.0.a1	*REV*	–	715.4214324	1,165.78228	1,677.928203
		ppe-miR171b	120.4938055	23.01315892	30.54025715	Prupe.5G072300_v2.0.a1	*SCL6*	Hypothetical protein	715.4214324	442.1932787	348.2492497
		ppe-miR171f	295.7575226	133.4763218	67.18856573	Prupe.5G072300_v2.0.a1	*SCL6*	Hypothetical protein	0	241.1963338	1,171.38384
		ppe-miR171h	635.3309746	211.7210621	24.43220572	Prupe.5G072300_v2.0.a1	*SCL6*	Hypothetical protein	715.4214324	442.1932787	348.2492497
		ppe-miR172a-3p	120.4938055	20.71184303	12.21610286	Prupe.6G091100_v2.0.a1	*RAP2-7*	–	37.6537596	200.9969448	284.9312043
						Prupe.6G231700_v2.0.a1	*AP2*	Uncharacterized LOC106378603	376.537596	1,045.184113	3,609.128588
						Prupe.6G242400_v2.0.a1	*AP2*	–	0	0	94.9770681
		ppe-miR172c	32.86194696	4.602631785	16.28813715	Prupe.6G091100_v2.0.a1	*RAP2-7*	–	37.6537596	200.9969448	284.9312043
						Prupe.6G231700_v2.0.a1	*AP2*	Uncharacterized LOC106378603	376.537596	1,045.184113	3,609.128588
						Prupe.6G242400_v2.0.a1	*AP2*	–	0	0	94.9770681

(to be continued)

Table 2. (continued)

GO_Id	GO_term	miRNA	DPA20_TPM	DPA50_TPM	DPA75_TPM	Transcript_ID	Symbol	Annoation	DPA20_TPM	DPA50_TPM	DPA75_TPM
		ppe-miR172d	65.72389392	2.301315892	4.072034287	Prupe.6G091100_v2.0.a1	*RAP2-7*	–	37.6537596	200.9969448	284.9312043
						Prupe.6G231700_v2.0.a1	*AP2*	Uncharacterized LOC106378603	376.537596	1,045.184113	3,609.128588
						Prupe.6G242400_v2.0.a1	*AP2*	–	0	0	94.9770681
		ppe-miR319a	164.3097348	29.9171066	171.02544	Prupe.3G124900_v2.0.a1	*TCP4*	–	37.6537596	0	63.3180454
						Prupe.4G083500_v2.0.a1	*TCP2*	–	75.3075192	80.39877794	664.8394767
						Prupe.4G171100_v2.0.a1	*PCF5*	–	112.9612788	0	94.9770681
		ppe-miR396a	6364.263728	59399.2645	71602.65089	Prupe.1G531300_v2.0.a1	*AGL24*	D-3-phosphoglycerate dehydrogenase	0	93.79857426	164.626918
GO:0045597	Positive regulation of cell differentiation	ppe-miR166a	18,358.87437	7,847.487193	3,273.915566	Prupe.1G447100_v2.0.a1	*ATHB-8*	–	414.1913556	2,170.767004	2,421.915237
GO:0051301	Cell division	ppe-miR160a	1,084.44425	333.6908044	177.1334915	Prupe.2G213000_v2.0.a1	*ARF18*	Auxin response factor 3	4,104.259796	9,286.058852	11,365.58915
						Prupe.6G102800_v2.0.a1	*ARF18*	Hypothetical protein	78,884.62636	112,477.8903	81,142.07518
						Prupe.6G236200_v2.0.a1	*ARF18*	Auxin response factor 3	10,806.629	33,566.48979	26,055.37568
		ppe-miR171b	120.4938055	23.01315892	30.54025715	Prupe.2G138400_v2.0.a1	*SCL6*	DELLA protein GAI 1	37.6537596	0	0
		ppe-miR171h	635.3309746	211.7210621	24.43220572	Prupe.2G138400_v2.0.a1	*SCL6*	DELLA protein GAI 1	37.6537596	0	0
GO:0008284	Positive regulation of cell proliferation	ppe-miR166a	18,358.87437	7,847.487193	3,273.915566	Prupe.1G447100_v2.0.a1	*ATHB-8*	–	414.1913556	2,170.767004	2,421.915237
GO:0008285	Negative regulation of cell proliferation	ppe-miR396a	6,364.263728	59,399.2645	71,602.65089	Prupe.1G419000_v2.0.a1	*GRF6*	–	1,242.574067	6,070.107734	4,558.899269
		ppe-miR396b	61,791.41427	484,650.223	540,299.9053	Prupe.1G419000_v2.0.a1	*GRF6*	–	1,242.574067	6,070.107734	4,558.899269
		ppe-miR396c	12,421.81595	118,018.3829	109,040.9341	Prupe.1G419000_v2.0.a1	*GRF6*	–	1,242.574067	6,070.107734	4,558.899269

Notably, some miRNAs were detected exclusively in one of the three developmental stages (Supplementary Table S4), suggesting that specific miRNAs may exhibit unique expression patterns during certain stages, enabling them to perform diverse regulatory functions in peach fruit development.

Target gene analysis of miRNAs in peach fruit

It has been proposed that plant miRNAs mediate gene expression mainly via miRNA-guided cleavage of target transcripts[51]. Therefore, identifying miRNA targets is a critical step in understanding the regulatory roles of miRNAs. In this study, degradome sequencing identified 216 cleaved targets for 74 known and eight novel miRNAs across the three developmental stages (Supplementary Table S5). Notably, the degradation levels of these targets varied across the three stages, suggesting that miRNAs may play distinct roles at different phases of peach fruit development. For example, the target genes of ppe-miR172a-3p, which encode *RAP2-7* and *AP2*, showed an increasing abundance of degradome tags as fruit development progressed. This indicates that *RAP2-7* and *AP2* are actively targeted by ppe-miR172a-3p during fruit development and ripening. Many conserved miRNA targets, particularly transcription factors, regulate diverse physiological processes, and genetic programs[47–50]. In this study, the majority of targets for peach miRNAs were also conserved. For instance, the miR156 family is known to target SQUAMOSA promoter binding protein-like (SPL) transcription factors[42,44]. In the present experiments, six SPL transcription factors genes were identified as targets of ppe-miR156a/c/f. Similarly, the miR166 family has highly conserved targets encoding class III homeodomain leucine zipper (HD-ZIP III) transcription factors, which are involved in various developmental processes across plant species[52–54]. We predicted that four HD-ZIP III family members are the targets of ppe-miR166a and except *ATHB-14*, the cleavage products of *REV*, *ATHB-8,* and *ATHB-15* are present in much greater quantities during FWII and FWIII than during FWI. This finding confirms that ppe-miR166a promotes late-stage development of fruits and may contribute to the fine-tuning of HD-ZIP III proteins. In addition to conserved targets, some miRNAs were found to have novel or additional targets in peach. For example, the miR396 family, known to target growth-regulating factor (GRF) genes, also targeted D-3-phosphoglycerate dehydrogenase, animal HSPA9 nucleotide-binding domain protein, and hypothetical proteins such as DAP and WEB1. Furthermore, 21 targets were detected for the eight novel miRNAs, many of which are involved in diverse biological processes. Specifically, 17 targets were identified for ppe-miR396a, including nine *GRF* genes, DNA topoisomerase 3-alpha, and other proteins. These findings suggest that miRNA-target interactions may exhibit species-specific characteristics during peach development.

Roles of miRNAs in peach fruit development

Auxin has long been considered a central regulator of ovary wall enlargement and pericarp development, and synthetic auxins have been shown to enhance fruit growth by stimulating fruit cell enlargement in peaches[54]. miRNAs have been shown to directly and indirectly regulate the auxin signaling pathway. For instance, the miR160 family targets auxin response factors (*ARF10*, *ARF16*, and *ARF17*) in multiple plant species[41,45,55], while the miR167 family regulates *ARF6* and *ARF8* to control reproductive processes[45,55]. Additionally, the miR393 family regulates the expression of the auxin receptor *TIR1* and related auxin signaling F-box proteins AFB1, AFB2,

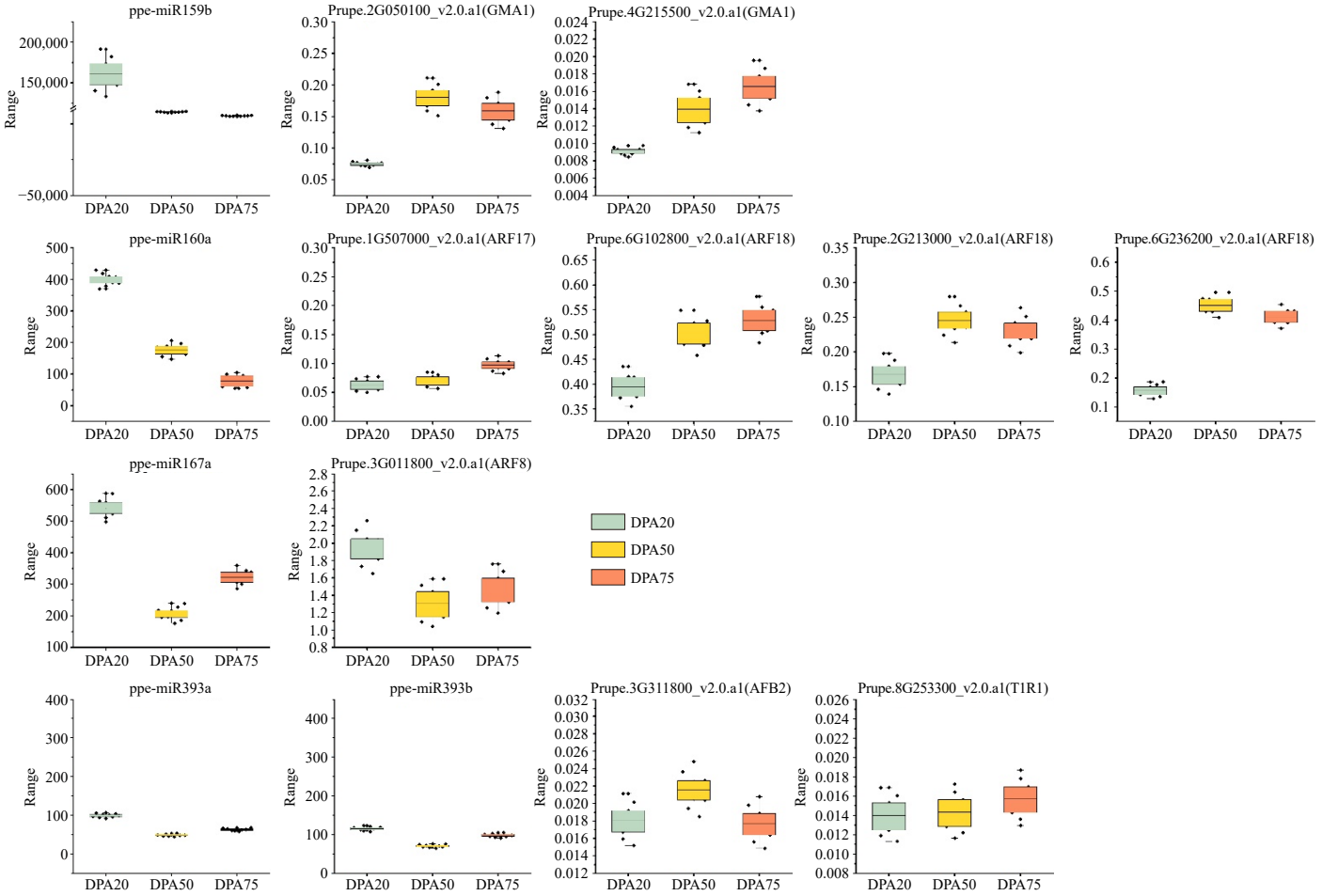

Fig. 6 Expression patterns of the four miRNAs identified and their target genes during fruit development and ripening; U6 and RPII were used as reference genes for miRNA and target genes, respectively.

and AFB3 in *Arabidopsis* and peaches[56]. In peaches, ppe-miR160a targets *ARF17* to regulate peach development during the hard-core stage[44], and the miR164 family negatively regulates a subset of NAC transcription factor family members, which are auxin-responsive and the key regulators of plant growth and development[57]. Our sequencing data show that ppe-miR160a, ppe-miR167a, ppe-miR393a/b, and ppe-miR164a/d regulate auxin signaling by targeting ARFs, auxin receptor *TIR1*, auxin signaling F-box proteins (*AFB2*), and NAC transcription factors (Fig. 7; Supplementary Table S5). Specifically, *ARF17* (Prupe.1G507000_v2.0.a1), *ARF18* (Prupe.6G102800_v2.0.a1, Prupe. 2G213000_v2.0.a1, and Prupe. 6G236200_v2.0.a1), and *ARF8* (Prupe.3G011800_v2.0.a1) were identified as targets gene of ppe-miR160a and ppe-miR167a, with cleavage products varying across developmental stages. These indicates that the targets of single miRNAs play different roles in peach developmental stages. Both ppe-miR393a and ppe-miR393b target the TIR1/AFB2 Auxin Receptor Clade (Table 2), as observed in *Arabidopsis*[56], but ppe-miR393b exhibited significantly stronger degradation effects on TIR1/AFB2 than ppe-miR393a across all stages. Furthermore, *NAC021*, a target of ppe-miR164a, was implicated in auxin signaling, with its cleavage products more abundant during FWII and FWIII than FWI. These findings collectively demonstrate that miRNAs regulate peach fruit development by modulating auxin signaling.

Fruit enlargement, a critical developmental process in peach and other fruiting plants, requires precise control of cell proliferation, expansion, and differentiation. To better understand the roles of miRNAs in peach enlargement, we analyzed miRNAs involved in cell proliferation and differentiation (Fig. 7; Table 2). For example, ppe-miR319c/e targets *TCP*s, which promote cell expansion and repress cell proliferation[58]. In our study, *TCP2* cleavage products were more abundant during FWIII than FWI and FWII (Supplementary Table S5). Additionally, ppe-miR396a targets *GRF*s were detected, and these have been previously shown to regulate the growth of citrus fruits and leaves[59]. We also confirmed conserved interactions, such as ppe-miR172 a-3p/c/d targeting *AP2* and ppe-miR166a targeting HD-ZIP III genes (*ATHB8*, *ATHB14*, *ATHB15*, and *REV*). In agreement, sl-miR172 targeting *SlAP2a* negatively regulated ethylene production during tomato ripening[60], and ppe-miR166a targeting the four HD-ZIP III subfamily genes *ATHB8*, *ATHB14*, *ATHB15*, and *REV* reportedly influences peach enlargement[44]. Notably, ppe-miR171b/f/h targeting *SCL6* was implicated in cell division, a novel finding not previously reported. The MADS-box protein, encoded by *AGL24* reportedly promotes flowering in *Arabidopsis* and was targeted by ppe-miR396a, which is also involved in cell differentiation (Fig. 7). Finally, ppe-miR160-*ARF* interactions, previously linked to fruit enlargement through auxin signaling, were also observed[44].

Conclusions

Using high-throughput RNA sequencing, we identified 124 conserved and 86 novel miRNAs in peach. Moreover, 216 sliced targets for 74 known and eight novel miRNAs were identified by degradome sequencing. Subsequent miRNA–gene–GO term

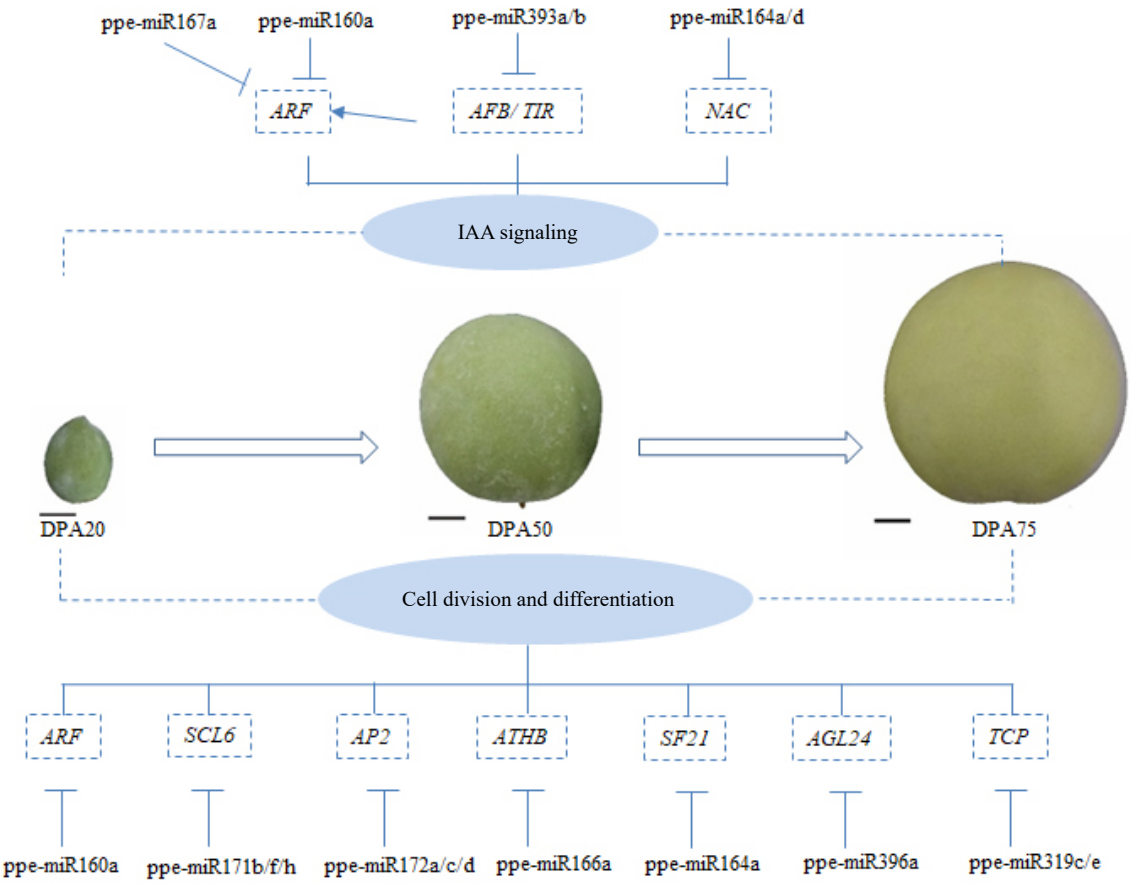

Fig. 7 A schematic model of the proposed roles of miRNAs in the early development of peaches; T bars and arrows refer to negative and positive effects on downstream effectors or biological process, respectively; scale bar = 1 cm

network analyses highlighted a complex miRNA regulatory network involved in auxin signaling, which plays a central role in peach enlargement (Fig. 5). Collectively, these findings provide a foundation for future studies on miRNA-mediated mechanisms underlying peach development.

Author contributions

The authors confirm contribution to the paper as follows: experiments conception and design: Zhang Y; experiments performing: Zhu X; data analysis: Wang C; manuscript writing: Zhang Y, Ge M. All authors reviewed the results and approved the final version of the manuscript.

Data availability

This transcriptome project has been deposited in the NCBI SRA (Sequence Read Archive) database (www.ncbi.nlm.nih.gov/sra). The BioProject ID related to this paper is SRP143921 (www.ncbi.nlm.nih.gov/sra/?term=SRP143921).

Acknowledgments

This work was supported by the Natural Science Foundation of Jiangsu (BK20201176 and BK20190542), Jiangsu University 'Qinglan Project' (2022). We thank Professor Chen Wang for her support and cooperation throughout this research.

Conflict of interest

The authors declare that they have no conflict of interest.

Supplementary information accompanies this paper at (https://www.maxapress.com/article/doi/10.48130/frures-0025-0010)

Dates

Received 15 March 2023; Revised 28 February 2025; Accepted 5 March 2025; Published online 26 May 2025

References

1. Zhan J, Meyers BC. 2023. Plant small RNAs: their biogenesis, regulatory roles, and functions. *Annual Review of Plant Biology* 74:21–51
2. Vaucheret H, Voinnet O. 2024. The plant siRNA landscape. *The Plant Cell* 36(2):246–75
3. Rogers K, Chen X. 2013. Biogenesis, turnover, and mode of action of plant microRNAs. *The Plant Cell* 25(7):2383–99
4. Navarro L, Dunoyer P, Jay F, Arnold B, Dharmasiri N, et al. 2006. A plant miRNA contributes to antibacterial resistance by repressing auxin signaling. *Science* 312:436–39
5. Krol J, Loedige I, Filipowicz W. 2010. The widespread regulation of microRNA biogenesis, function and decay. *Nature Reviews Genetics* 11(9):597–610
6. Xie F, Jones DC, Wang Q, Sun R, Zhang B. 2015. Small RNA sequencing identifies miRNA roles in ovule and fibre development. *Plant Biotechnology Journal* 13(3):355–69
7. Farooq M, Mansoor S, Guo H, Imran A, Chee, et al. 2017. Identification and characterization of miRNA transcriptome in asiatic cotton (*Gossypium arboreum*) using high throughput sequencing. *Frontiers in Plant Science* 8:969
8. Liu M, Yu H, Zhao G, Huang Q, Lu Y, et al. 2017. Profiling of drought-responsive microRNA and mRNA in tomato using high-throughput sequencing. *BMC Genomics* 18(1):481

9. Liu M, Yu H, Zhao G, Huang Q, Lu Y, et al. 2018. Identification of drought-responsive microRNAs in tomato using high-throughput sequencing. *Functional & Integrative Genomics* 18(1):67−78
10. Ferigolo LF, Vicente MH, Correa JPO, Barrera-Rojas CH, Silva EM, et al. 2023. Gibberellin and miRNA156-targeted SlSBP genes synergistically regulate tomato floral meristem determinacy and ovary patterning. *Development* 150(21):dev201961
11. Wang C, Jogaiah S, Zhang W, Abdelrahman M, Fang JG. 2018. Spatio-temporal expression of *miRNA159* family members and their *GAMYB* target gene during the modulation of gibberellin-induced grapevine parthenocarpy. *Journal of Experimental Botany* 69(15):3639−50
12. Li D, Mou W, Luo Z, Li L, Limwachiranon J, et al. 2016. Developmental and stress regulation on expression of a novel miRNA, Fan-miR73, and its target ABI5 in strawberry. *Scientific Reports* 6:28385
13. Meyers BC, Axtell MJ. 2019. MicroRNAs in plants: key findings from the early years. *The Plant Cell* 31(6):1206−07
14. Azad MF, Dawar P, Esim N, Rock CD. 2023. Role of miRNAs in sucrose stress response, reactive oxygen species, and anthocyanin biosynthesis in *Arabidopsis thaliana*. *Frontiers in Plant Science* 14:1278320
15. Qu D, Yan F, Meng R, Jiang X, Yang H, et al. 2016. Identification of MicroRNAs and their targets associated with fruit-bagging and subsequent sunlight re-exposure in the "Granny Smith" apple exocarp using high-throughput sequencing. *Frontiers in Plant Science* 7:27
16. Zhao F, Wang C, Han J, Zhu X, Li X, et al. 2017. Characterization of miRNAs responsive to exogenous ethylene in grapevine berries at whole genome level. *Functional & Integrative Genomics* 17(2-3):213−35
17. Guo DL, Li Q, Lv WQ, Zhang GH, Yu YH. 2018. MicroRNA profiling analysis of developing berries for 'Kyoho' and its early-ripening mutant during berry ripening. *BMC Plant Biology* 18(1):285
18. Zhu H, Xia R, Zhao B, An Y, Dardick CD, et al. 2012. Unique expression, processing regulation, and regulatory network of peach (*Prunus persica*) miRNAs. *BMC Plant Biology* 12:149
19. Zhang Y, Bai Y, Han J, Chen Ming, Kayesh E, et al. 2013. Bioinformatics prediction of miRNAs in the *Prunus persica* genome with validation of their precise sequences by miR-RACE. *Journal of Plant Physiology* 170(1):80−92
20. Saminathan T, Bodunrin A, Singh NV, Devarajan R, Nimmakayala P, et al. 2016. Genome-wide identification of microRNAs in pomegranate (*Punica granatum* L.) by high-throughput sequencing *BMC Plant Biology* 16(1):122
21. Xin C, Liu W, Lin Q, Zhang X, Cui P, et al. 2015. Profiling microRNA expression during multi-staged date palm (*Phoenix dactylifera* L.) fruit development. *Genomics* 105(4):242−51
22. Wu J, Zheng S, Feng G, Yi H. 2016. Comparative analysis of miRNAs and their target transcripts between a spontaneous late-ripening sweet orange mutant and its wild-type using small RNA and degradome sequencing. *Frontiers in Plant Science* 7:1416
23. Hou Y, Zhai L, Li X, Xue Y, Wang J, et al. 2017. Comparative analysis of fruit ripening-related miRNAs and their targets in blueberry using small RNA and degradome sequencing. *International Journal of Molecular Sciences* 18(12):2767
24. Lowenstein DM, Minor ES. 2016. Diversity in flowering plants and their characteristics: integrating humans as a driver of urban floral resources. *Urban Ecosystems* 19:1735−48
25. Tani E, Tsaballa A, Stedel C, Kalloniati C, Papaefthimiou D, et al. 2011. The study of a *SPATULA*-like bHLH transcription factor expressed during peach (*Prunus persica*) fruit development. *Plant Physiology and Biochemistry* 49(6):654−63
26. Jung S, Staton M, Lee T, Blenda A, Svancara R, et al. 2008. GDR (Genome Database for Rosaceae): integrated web-database for Rosaceae genomics and genetics data. *Nucleic Acids Research* 36:D1034−D1040
27. Veerappan K, Natarajan S, Chung H, Park J. 2021. Molecular insights of fruit quality traits in peaches, *Prunus persica*. *Plants* 10(10):2191
28. Esmaeili F, Shiran B, Fallahi H, Mirakhorli N, Budak H, et al. 2017. In silico search and biological validation of microRNAs related to drought response in peach and almond. *Functional & Integrative Genomics* 17:189−201
29. Gao Z, Luo X, Shi T, Cai B, Zhang Z, et al. 2012. Identification and validation of potential conserved microRNAs and their targets in peach (*Prunus persica*). *Molecules and Cells* 34(3):239−50
30. Luo X, Gao Z, Shi T, Cheng Z, Zhang Z, et al. 2013. Identification of miRNAs and their target genes in peach (*Prunus persica* L.) using high-throughput sequencing and degradome analysis. *PLoS One* 8:e79090
31. Quan W, Liu B, Wang Y. 2021. Fast and SNP-aware short read alignment with SALT. *BMC Bioinformatics* 22(Suppl 9):172
32. Wen M, Shen Y, Shi S, Tang T. 2012. miREvo: an integrative microRNA evolutionary analysis platform for next-generation sequencing experiments. *BMC Bioinformatics* 13:140
33. Friedländer MR, Mackowiak SD, Li N, Chen W, Rajewsky N. 2012. miRDeep2 accurately identifies known and hundreds of novel microRNA genes in seven animal clades. *Nucleic Acids Research* 40(1):37−52
34. Tang Y, Ghosal S, Roy A. 2007. Nonparametric bayesian estimation of positive false discovery rates. *Biometrics* 63(4):1126−34
35. Addo-Quaye C, Miller W, Axtell MJ. 2009. CleaveLand: a pipeline for using degradome data to find cleaved small RNA targets. *Bioinformatics* 25(1):130−31
36. Kohl M, Wiese S, Warscheid B. 2011. Cytoscape: software for visualization and analysis of biological networks. In *Data Mining in Proteomics*, eds Hamacher M, Eisenacher M, Stephan C. US: Humana Press. Volume 696. pp. 291−303. doi: 10.1007/978-1-60761-987-1_18
37. Shangguan L, Song C, Han J, Leng X, Kibet KN, et al. 2014. Characterization of regulatory mechanism of *Poncirus trifoliata* microRNAs on their target genes with an integrated strategy of newly developed PPM-RACE and RLM-RACE. *Gene* 535(1):42−52
38. Tiwari B, Habermann K, Arif MA, Top O, Frank W. 2021. Identification of small RNAs during high light acclimation in *Arabidopsis thaliana*. *Frontiers in Plant Science* 12:656657
39. Varkonyi-Gasic E. 2017. Stem-loop qRT-PCR for the detection of plant microRNAs. In *Plant Epigenetics*, ed. Kovalchuk I. Boston, MA: Humana Press.Volume 1456. pp. 163−75. doi: 10.1007/978-1-4899-7708-3_13
40. Pasquinelli AE. 2012. MicroRNAs and their targets: recognition, regulation and an emerging reciprocal relationship. *Nature Review Genetics* 13(4):271−82
41. Dai X, Lu Q, Wang J, Wang L, Xiang F, et al. 2021. MiR160 and its target genes *ARF10*, *ARF16* and *ARF17* modulate hypocotyl elongation in a light, BRZ, or PAC-dependent manner in Arabidopsis: miR160 promotes hypocotyl elongation. *Plant Science* 303:110686
42. de Sousa Cardoso TC, Alves TC, Caneschi CM, dos Reis Gomes Santana D, Fernandes-Brum CN, et al. 2018. New insights into tomato microRNAs. *Science Reports* 8(1):16069
43. Li BJ, Bao RX, Shi YN, Grierson D, Chen KS. 2024. Auxin response factors: important keys for understanding regulatory mechanisms of fleshy fruit development and ripening. *Horticulture Research* 11(10):uhae209
44. Shi M, Hu X, Wei Y, Hou X, Yuan X, et al. 2017. Genome-wide profiling of small RNAs and degradome revealed conserved regulations of miRNAs on auxin-responsive genes during fruit enlargement in peaches. *International Journal of Molecular Science* 18(12):2599
45. Zimmerman K, Pegler JL, Oultram JMJ, Collings DA, Wang MB, et al. 2024. Molecular manipulation of the miR160/*AUXIN RESPONSE FACTOR* expression module impacts root development in *Arabidopsis thaliana*. *Genes* 15(8):1042
46. Wang Y, Li W, Chang H, Zhou J, Luo Y, et al. 2020. SRNAome and transcriptome analysis provide insight into strawberry fruit ripening. *Genomics* 112(3):2369−78
47. Tang J, Chu C. 2017. MicroRNAs in crop improvement: fine-tuners for complex traits. *Nature Plants* 3:17077
48. Samad AFA, Sajad M, Nazaruddin N, Fauzi IA, Murad AM, et al. 2017. MicroRNA and transcription factor: key players in plant regulatory network. *Frontiers in Plant Science* 8:565
49. Zhang H, Yin L, Wang H, Wang G, Ma X, et al. 2017. Genome-wide identification of Hami melon miRNAs with putative roles during fruit development. *PLoS One* 12(7):e0180600
50. Cui J, You C, Chen X. 2017. The evolution of microRNAs in plants. *Current Opinion in Plant Biology* 35:61−67
51. Sun YH, Lu S, Shi R, Chiang VL. 2011. Computational prediction of plant miRNA targets. In *RNAi and Plant Gene Function Analysis*, eds Kodama H, Komamine A. US: Humana Press. Volume 744. pp. 175−86. doi: 10.1007/978-1-61779-123-9_12

52. Yadav A, Kumar S, Verma R, Lata C, Sanyal I, et al. 2021. microRNA 166: an evolutionarily conserved stress biomarker in land plants targeting HD-ZIP family. *Physiology and Molecular Biology of Plants* 27:2471–85
53. Jia X, Ding N, Fan W, Yan J, Gu Y, et al. 2015. Functional plasticity of miR165/166 in plant development revealed by small tandem target mimic. *Plant Science* 233:11–21
54. Ma L, Zhao Y, Chen M, Li Y, Shen Z, et al. 2023. The microRNA ppe-miR393 mediates auxin-induced peach fruit softening by promoting ethylene production. *Plant Physiology* 192(2):1638–55
55. Gaddam SR, Sharma A, Bhatia C, Trivedi PK. 2024. A network comprising ELONGATED HYPOCOTYL 5, microRNA397b, and auxin-associated factors regulates root hair growth in Arabidopsis. *Plant Physiology* 196(2):1460–74
56. Jiang J, Zhu H, Li N, Batley J, Wang Y. 2022. The miR393-target module regulates plant development and responses to biotic and abiotic stresses. *International Journal of Molecular Sciences* 23(16):9477
57. Wang J, Li R, Chen Y, Wang X, Shi Q, et al. 2023. Expressing a Short Tandem Target Mimic (STTM) of miR164b/e-3p enhances poplar leaf serration by co-regulating the miR164-*NAC* module. *Plant Physiology and Biochemistry* 201:107790
58. Karidas P, Challa KR, Nath U. 2015. The *tarani* mutation alters surface curvature in *Arabidopsis* leaves by perturbing the patterns of surface expansion and cell division. *Journal of Experimental Botany* 66(7):2107–22
59. Liu X, Guo LX, Jin LF, Liu YZ, Liu T, et al. 2016. Identification and transcript profiles of citrus growth-regulating factor genes involved in the regulation of leaf and fruit development. *Molecular Biology Reports* 43(10):1059–67
60. Chung MY, Nath UK, Vrebalov J, Gapper N, Lee JM, et al. 2020. Ectopic expression of miRNA172 in tomato (*Solanum lycopersicum*) reveals novel function in fruit development through regulation of an *AP2* transcription factor. *BMC Plant Biology* 20(1):283

Copyright: © 2025 by the author(s). Published by Maximum Academic Press, Fayetteville, GA. This article is an open access article distributed under Creative Commons Attribution License (CC BY 4.0), visit https://creativecommons.org/licenses/by/4.0/.